TISSUE ENGINEERING: Part A
Volume 00, Number 00, 2025

DOI: 10.1177/19373341251369772

termis
Tissue Engineering
& Regenerative Medicine
International Society

***ORIGINAL ARTICLE***

# Human Recellularization for Xenoantigen-Free Decellularized Cardiac Xenografts

Ja-Kyoung Yoon, MD,[1] So Young Kim,[2] Serin Kim,[2] Kyung Mee Lee,[2] Sunhi Ko,[2] Gi Beom Kim, MD, PhD,[3] Hong-Gook Lim, MD, PhD,[2] and Yong Jin Kim, MD, PhD[4]



Removal of major xenoantigens of the Galα1-3Gal (α-Gal) epitope and the nonhuman sialic acid *N*-glycolylneuraminic acid (Neu5Gc) is essential to eliminate xenoimmunogenicity and optimize recellularization for cardiac xenografts. The aim of this study was to evaluate the safety and efficacy of α-galactosidase for removal of α-Gal xenoantigen and peptide *N*-glycosidase F (PNGase-F) for removal of non-α-Gal xenoantigen combined with optimal decellularization, and the potential of *in vitro* recellularization was assessed with coculturing human mesenchymal stem cells and human umbilical vein endothelial cells for major xenoantigen-free cardiac xenografts. We investigated the biomechanical properties and efficacy for xenoantigen removal with expression of carbohydrate-binding lectins in porcine pericardia decellularized and treated with α-galactosidase and PNGase-F. There were no histological changes depending on α-galactosidase and PNGase-F treatment. There was no difference in tensile stress, tensile displacement, tensile strain at break, and permeability test following enzymatic treatments. Both enzyme-treated xenografts were stained with Jacalin, Maackia amurensis lectin I, wheat germ agglutinin, Ricinus communis agglutinin, Griffonia simplicifolia lectin (GSL), erythrina cristagalli lectin, peanut agglutinin, soybean agglutinin, Wisteria floribunda lectin, and Datura stramonium lectin and showed synergistic effects for low fluorescence qualitatively and quantitatively. The enzymatic treatments for decellularization significantly reduced lectin expression, demonstrating the synergistic effect of both enzymes and decellularization. *In vitro* recellularization for decellularized and both enzymes-treated xenografts was assessed with vimentin, calponin, fibronectin, and CD31 staining. Stronger signals were detected in decellularized xenografts, and decellularized xenografts treated with both enzymes showed significantly faster mesenchymal cell infiltration into the tissue, leading to accelerated recellularization. We have successfully produced major xenoantigen-free scaffolds by demonstrating the safety and the synergistic effect of α-galactosidase and PNGase-F treatments and proved effective recellularization for the xenoantigen-free scaffolds not previously reported in the literature.

**Keywords:** tissue engineering, decellularization, recellularization

### Impact Statement

We identified a method for *in vitro* recellularization using major xenoantigen-free cardiac xenografts processed according to our previous optimized decellularization protocol. The safety and efficacy for optimal decellularization combined with α-galactosidase for removal of α-Gal xenoantigen and PNGase-F for removal of non-α-Gal xenoantigen were demonstrated. The effective recellularization was proved with coculturing human mesenchymal stem cells and human umbilical vein endothelial cells for cardiac xenograft scaffolds with reduced immunogenicity and enhanced biocompatibility for the first time in the world.

[1]Department of Pediatrics, Samsung Medical Center, Sungkyunkwan University School of Medicine, Seoul, South Korea.
[2]Department of Thoracic and Cardiovascular Surgery, Seoul National University Hospital, Seoul National University College of Medicine, Seoul, South Korea.
[3]Department of Pediatrics, Seoul National University Hospital, Seoul National University College of Medicine, Seoul, South Korea.
[4]Department of Thoracic and Cardiovascular Surgery, Sejong General Hospital, Bucheon, South Korea.

## Introduction

Finding an ideal heart valve is a critical issue in treating patients with heart disease, especially for those with congenital heart disease who had disease specifically related to right ventricular outflow tract abnormalities, because they require repeated reoperations as they grow older. The ideal xenogeneic valve should be nonthrombogenic, nonimmunogenic, durable, and have the potential to grow. Xenogeneic decellularized heart valves have been extensively studied as an attractive alternative for the development of viable biological valves capable of remodeling and regeneration. Decellularization protocols included a process to remove the cellular components of the original tissue while preserving the three-dimensional extracellular matrix (ECM) of the biological tissue.[1] Although a consensus on decellularization protocols has not yet been reached, we previously developed an optimal decellularization protocol using sodium dodecyl sulfate (SDS) and Triton X-100 through a multistep method with hypotonic, isotonic, and hypertonic buffer solutions.[2–4] This protocol has been shown to preserve the microstructure, the degree of cross-linking, and tissue strength; reduce cytotoxicity; and inhibit *in vivo* calcification of glutaraldehyde (GA)-fixed xenografts. To remove major xenoantigens of the Gal$\alpha$1-3Gal ($\alpha$-Gal) responsible for hyperacute graft rejection upon transplantation in humans, we developed $\alpha$-Gal-free cardiac xenografts treated with optimal decellularization and $\alpha$-galactosidase and succeeded in clinical application and commercialization.[5–7] However, the $\alpha$-Gal-free decellularized tissues developed in this way still elicit tissue reactions in the body, leading to calcification and degeneration, because of the major xenoantigens of the nonhuman sialic acid *N*-glycolylneuraminic acid (Neu5Gc). The Neu5Gc are responsible for acute graft rejection upon transplantation in humans, and peptide *N*-glycosidase F (PNGase-F) for the reduction in glycans from cardiac xenografts can attenuate the immunogenicity of xenogeneic scaffolds.

There is a significant clinical need for valve tissues that can prevent degeneration, provide growth characteristics, and reduce the replacement cycle, particularly for pediatric patients. The recellularization of decellularized xenografts is believed to have the potential to shift xenoreactive immune responses toward an anti-inflammatory phenotype and enhance cellular regeneration, making it a promising candidate for an ideal valve tissue.

In this study, we aimed to identify a method for *in vitro* recellularization using major xenoantigen-free cardiac xenografts processed according to our previous optimized decellularization protocol. The safety and efficacy for optimal decellularization combined with $\alpha$-galactosidase for removal of $\alpha$-Gal xenoantigen and PNGase-F for removal of non-$\alpha$-Gal xenoantigen were evaluated, and the potential of *in vitro* recellularization was assessed with coculturing human mesenchymal stem cells (MSCs) and human umbilical vein endothelial cells (HUVECs) for cardiac xenograft scaffolds with reduced immunogenicity and enhanced biocompatibility.

## Materials and Methods

### *Tissue preparation and decellularization*

This study was approved by the Institutional Animal Care and Use Committee of Clinical Research Institute, Seoul National University Hospital (IACUC No. 24-0081-S1A0). Porcine pericardia were obtained from Taewoong Medical Inc., (South Korea). After fat and connective tissue removal on the surface of pericardium, these tissues were trimmed. The tissues were sterilized with 0.1% PAA for 4 h at room temperature (RT) and then washed with phosphate buffered saline solution (PBS) under agitation at RT. The porcine pericardium was directly decellularized using various solutions. Each process of decellularization was carried out under an agitator (180 rpm) in an orbital shaker (SHO-2D, DAIHAN).

The porcine pericardial tissues were initially decellularized with hypotonic solution for 14 h at 4°C and hypotonic solution with 0.25% SDS (Sigma, 436143) in di$H_2O$ containing 0.5% (v/v) Triton X-100 for 24 h at 4°C while agitating, and then washed with distilled water for 12 h at 4°C. After washing, these tissues were decellularized with isotonic solution for 48 h at 4°C. The tissues were treated in PBS with 30% polyethylene glycol 1000 and 1% antibiotic/antimycotic for 48 h, using an agitator at 4°C. The tissues were finally treated with a hypertonic solution for 3 h at 4°C. The tissues were washed in PBS for 24 h. Decellularized samples were prepared by our decellularization protocols as described by Lim HG, et al.[2]

### *Enzymatic digestion*

Native and decellularized porcine pericardia were treated with PNGase-F (#P0704L, 1000U, NEB) to obtain PNGase-F concentrations of 500, 1000, 1500, and 2000 unit/mL. In addition, native and decellularized porcine pericardia were treated with recombinant $\alpha$-galactosidase (G7163, Sigma) to obtain recombinant $\alpha$-galactosidase concentrations of 0.1 and 0.2 unit/mL. Native tissues served as an untreated control or negative control. Native and SDS + Triton X-100 (Tx)-decellularized porcine pericardia were treated with different enzymatic treatments: $\alpha$-galactosidase, PNGase-F, or $\alpha$-galactosidase in combination with PNGase-F. The sliced porcine pericardial tissues of $5 \times 5$ mm size in tubes with isotonic solution were conducted for 24 h in 4°C with agitation. Each enzymatic digestion with sliced tissues was treated at 37°C for 24 h under agitation, and then the tissues were rinsed in PBS under agitation (120 rpm) at RT. Finally, the tissue samples were stored in sterile PBS supplemented with 1% (v/v) penicillin/streptomycin and 400 $\mu$L/L amphotericin B for 24 h at 4°C.

### *Biomechanical analysis*

After enzymatic digestions, all samples were stored at 4°C for 24 h and then rinsed in PBS. Biomechanical analyses were performed on native pericardium with or without enzymatic treatments. According to manufacturer's instruction, the sliced samples were cut into approximately $5.0 \times 20$ mm (test length $\times$ width, $n = 30$), and the tensile strength was measured for a width of 5 mm. Thickness of pericardium tissue was determined at three points of the pieces using a thickness gauge (Quick-Mini 700-117; Mitutoyo, Kawasaki, Japan). Tensile properties were performed using an Instron tensile testing machine (68SC-5, INSTRON, USA) (100 N load cell) used to evaluate whether a difference existed in the maximal tensile strength of each sample, as described by Nam et al.[3] Ultimate strength and strain behaviors of each sample were analyzed by means of the following three

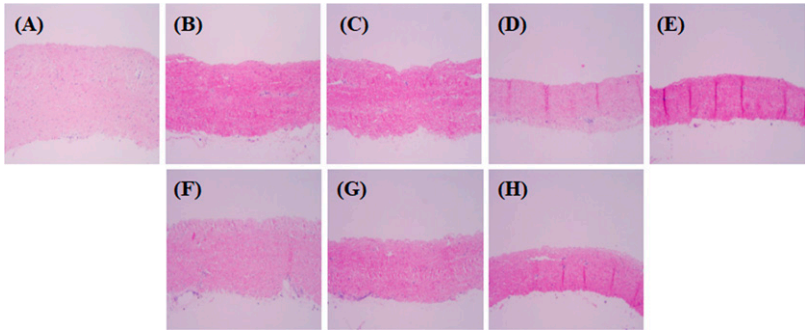


**FIG. 1.** Histological observation of native, α-galactosidase, and PNGase-F-treated group. **(A–H)** The porcine pericardium was treated with or without 0–2000 unit/mL PNGase-F, respectively, in the absence and presence of α-galactosidase (0.1–0.2 unit/mL) for 24 h. Native **(A)**, PNGase-F 500 **(B)**, PNGase-F 1000 **(C)**, PNGase-F 1500 **(D)**, PNGase-F 2000 **(E)**, α-galactosidase 0.1 **(F)**, α-galactosidase 0.2 **(G)**, and α-galactosidase 0.1 + PNGase-F 1000 **(H)** porcine pericardium samples were stained with H&E. H&E stains were imaged using a microscope. The magnification used was ×200.

parameters such as: tensile strain, maximum force, and tensile displacement. Permeability properties were determined by measuring the penetrated amounts of saline solution and applying constant pressure of 100 mmHg with saline on the pericardial tissues for 1 h, as described by Nam et al.[3] For this test, the tissues were cut into rectangular pieces approximately 1 $cm^2$ ($n = 8$).

### *Histology and lectin histochemistry for staining*

For histological staining, native and SDS + Tx-decellularized porcine pericardia were treated with different enzymatic treatments: α-galactosidase, PNGase-F, or α-galactosidase in combination with PNGase-F, and these sliced samples were fixed at 4% paraformaldehyde for 24 h in 4°C. Histological sections

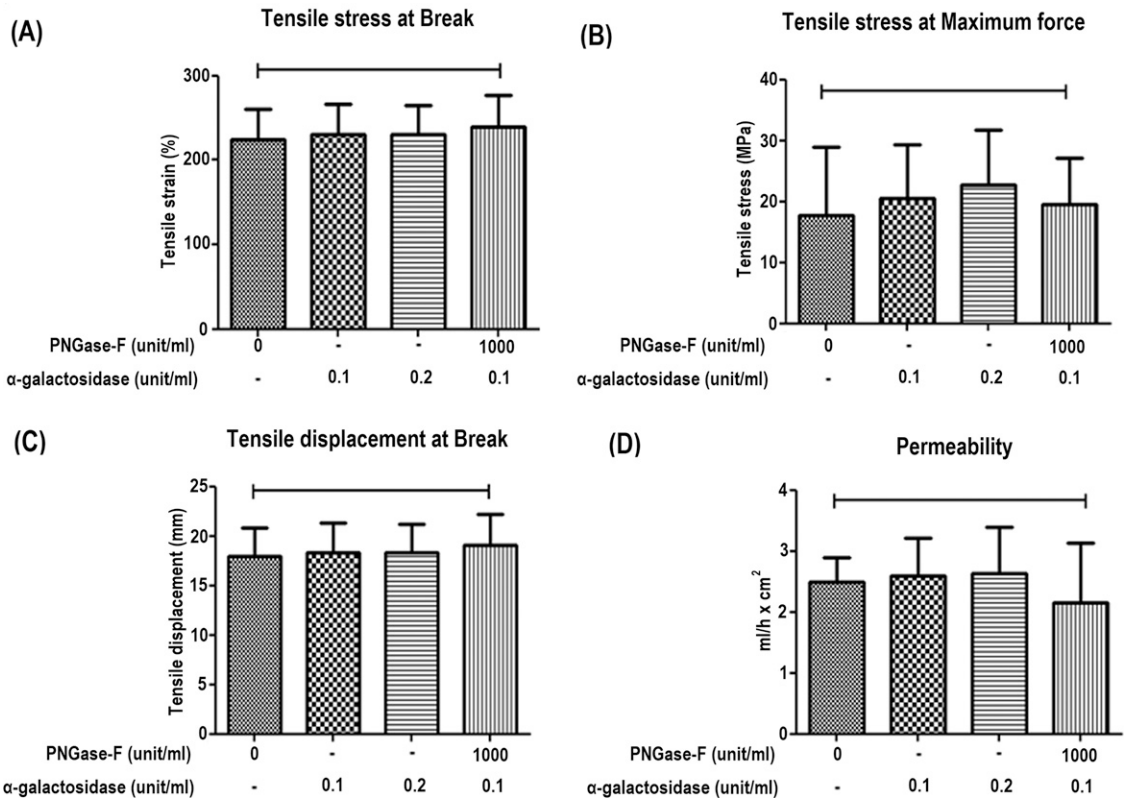


**FIG. 2.** Biomechanical properties of the native, α-galactosidase, and PNGase-F-treated group. **(A–D)** Tissue samples include native tissue and enzymatic treated tissue. The porcine pericardium was treated with or without 0–1000 unit/mL PNGase-F, respectively, in the absence and presence of α-galactosidase (0.1–0.2 unit/mL) for 24 h. **(A–C)** Uniaxial tensile mechanical analysis of porcine was pericardium analyzed using a tensile testing machine. Graph **(A)**, tensile stress at break; Graph **(B)**, tensile stress at maxium force; Graph **(C)**, tensile displacement at Break. **(D)** Permeability analysis of porcine pericardium analyzed using a permeability testing machine. Data represent the mean ± SD. Statistical significance was calculated using one-way analysis of variance with Dunnett's multiple comparisons test. $*p < 0.05$, $**p < 0.01$, $****p < 0.0001$.

(5 $\mu$m) of each sample were stained for hematoxylin and eosin (H&E) and lectins staining. The tissue sections were incubated with lectins at 1:250 overnight at 4°C. Effects of the enzymatic treatments on carbohydrate-binding lectins such as isolectin B4 (IL-B4/GSL-IB4) (#B-1205, Vector Laboratories Inc), specific for α-galactose residues; Wheat Germ Agglutinin (WGA) (#RL-1022, Vector Laboratories Inc); Datura Stramoniumlectin (DSL) (#B-1185, Vector Laboratories Inc); Ricinus Communis Agglutinin I (RCA-I) (#RL-1082, Vector Laboratories Inc); Soybean Agglutinin (SBA) (#B-1015, Vector Laboratories Inc); Wisteria Floribunda Lectin (WFA) (#B-1355, Vector Laboratories Inc); Peanut Agglutinin (PNA) (#B-1075, Vector Laboratories Inc); Maackia Amurensis lectin I (MAL I) (#B-1315, Vector Laboratories Inc); Jacalin (#B-1155, Vector Laboratories Inc); Erythrina Cristagalli Lectin (ECA) (#B-1145, Vector Laboratories Inc). Stained sections were additionally stained with avidin-linked Texas Red (#A-2006; Vector Laboratories Inc). The sections were washed 3 times with PBS, and stained sections were imaged using an inverted fluorescence microscope (DMI4000B, Leica, Germany). Stained images were obtained using Application Suite X Image Viewer (Leica).



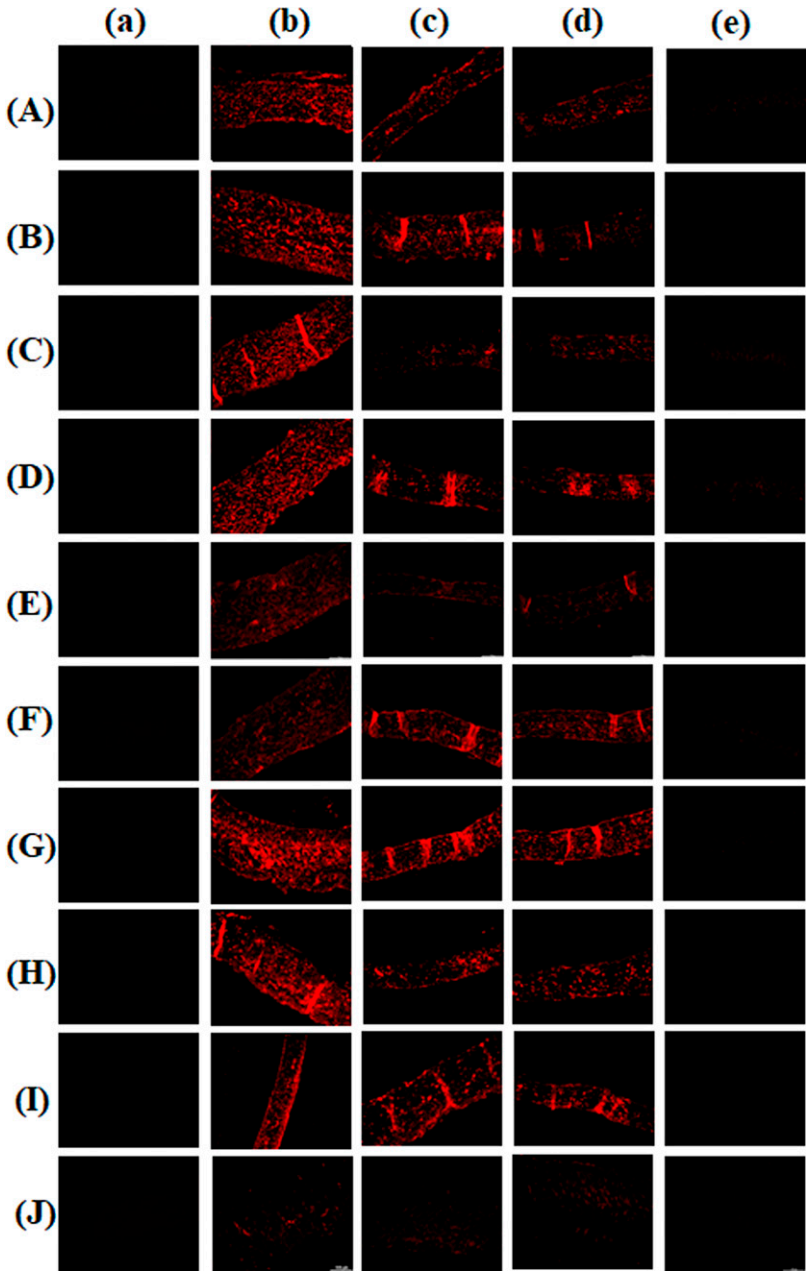


**FIG. 3.** Lectin histochemistry of native, α-galactosidase, and PNGase-F-treated group. **(a–e)** The porcine pericardium was treated with or without 0–1000 unit/mL PNGase-F, respectively, in the absence and presence of α-galactosidase (0.1–0.2 unit/mL) for 24 h. Negative control **(a)** from native tissue, native **(b)**, α-galactosidase 0.1 **(c)**, α-galactosidase 0.2 **(d)**, and α-galactosidase 0.1 + PNGase-F 1000 **(e)** porcine pericardium samples were cut longitudinally and stained with Jacalin **(A)**, MAL-I **(B)**, WGA **(C)**, RCA-I **(D)**, GSL **(E)**, ECA **(F)**, PNA **(G)**, SBA **(H)**, WFA **(I)**, and DSL **(J)**. Each sample of carbohydrate-binding lectins was stained red. The magnification used was ×200.

### *Lectin binding assay*

Lectin binding analysis was determined for porcine pericardial tissues with or without enzymatic treatments: α-galactosidase, PNGase-F, or α-galactosidase in combination with PNGase-F, and these sliced samples were homogenized in Radio-Immunoprecipitation Assay (RIPA) lysis buffer (ATTO) and stored in frozen condition. Tissue homogenates were coated onto a 96-well plate (Corning) in duplicates with coating buffer (Biosesang), and incubated overnight at 4°C, and then each wells was blocked with carbo-free blocking solution (#SP-5040-125, Vector Laboratories Inc.) for 1 h at RT. Wells were aspirated and incubated with diluted primary lectins (1:500) at 100 $\mu$L per well in the carbo-free blocking solution for 3 h at RT. After the primary lectins incubation, the plates were washed 3 times with PBS containing 0.05% Tween 20 (PBST, Biosesang). Subsequently, the wells were incubated for 30 min at RT with streptavidin-conjugated peroxidise (1:1000, #SA-S0004, Vector Laboratories Inc.) in blocking solution. Following several washes with PBST, the reaction was developed with a 3,3′,5,5′-tetrame-thylbenzidine (TMB) solution (#34028, Thermo Scientific). The absorbance of lectins was measured at 450 nm using an ELISA reader (TECAN, Spark).

### In vitro *culture and expansion of HUVECs and human adipose tissue-derived stem cells (ADSCs)*

HUVECs (#C2517A, Lonza) were purchased from ATCC (PCS-100-010, USA). HUVECs were used as pooled primary cells frozen after the first subculture. HUVECs were cultured at 37°C in a humidified atmosphere of 5% $CO_2$ with Endothelial Growth Medium-2 BulletKit$^{TM}$ (EGM, CC-3162, Lonza). Human ADSCs were purchased from Thermo Scientifics (#R7788115, USA). ADSCs were cultured at 37°C in a humidified atmosphere of 5% $CO_2$ with Dulbecco's Modified Eagle Medium (DMEM) medium containing 10% fetal bovine serum (FBS), transforming growth factor beta 1 (TGF-$\beta$1, 2.5 ng/mL, ab50036, Abcam), and bone morphogenetic protein 4 (BMP-4, 2.5 ng/mL, SRP6156, Sigma). The cell culture medium of both cells was changed every 3 days.

### *Pericardium modification*

For recellularization, modification of porcine pericardium was performed on native, decellularized, and decellularized porcine pericardium treated with α-galactosidase in combination with PNGase-F. The pericardial samples were cut into approximately 1 × 1 cm (length × width, $n = 3$), and the sliced pericardial samples were coated with a fibrin mesh (P- or DP-Fb) in a 12-well plates. The samples were washed with 0.05 M Tris-HCl buffer (TB) solution, and it was modified by attachment of heparin (P- or DP-Fb + H) overnight at 4°C, and then the fibrin mesh + heparin (P- or DP-Fb + H) samples were washed with PBS, and they were incubated with vascular endothelial growth factor (VEGF 165, 100 ng/mL in PBS, GeneScript USA Inc.) for 2 h at RT and were rinsed with PBS, as described by Filova et al.[8]

### *ADSCs and HUVECs seeded onto modified pericardium (HUVECs/ADSCs coculture)*

For endothelialization of the pericardium, all pericardial samples were seeded on both sides with ADSCs and HUVECs coculture. ADSCs (passage 3) were seeded on top of all modified pericardial samples (P- or DP-Fb + H + VEGF) at

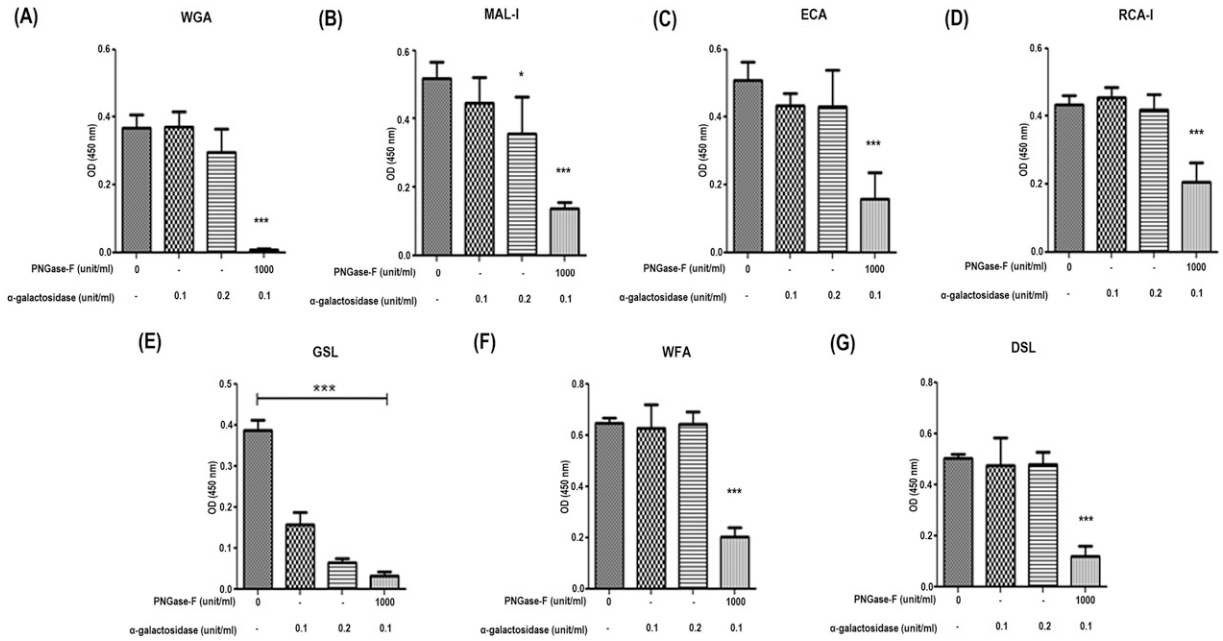


**FIG. 4.** Quantitative evaluation of lectins binding to solubilized proteins of porcine pericardium. The porcine pericardium was treated with or without 0–1000 unit/mL PNGase-F, respectively, in the absence and presence of α-galactosidase (0.1–0.2 unit/mL) for 24 h. Each tissue samples were homogenized with lysis buffer, and detection of lectin-binding to solubilized extracellular matrix proteins on the surface of the tissue was performed to detect the expression of WGA (**A**), MAL-I (**B**), ECA (**C**), RCA-I (**D**), GSL (**E**), WFA (**F**), and DSL (**G**). Each sample was determined in triplicates. The graphs show the quantification results. Data are represented as mean ± SD of five independent experiments. Statistical significance was calculated using one-way analysis of variance with Dunnett's multiple comparisons test. $*p < 0.05$, $**p < 0.01$, $***p < 0.001$.

approximately $1 \times 10^5$ cells (day 0) per well in a 12-well plate. The seeded samples were turned over, and ADSCs were seeded on the bottom of samples in DMEM medium supplemented with 2% FBS, TGF-$\beta$1, and BMP-4 (day 2). After ADSCs seeding on both sides, subsequently, HUVECs (passage 6) were seeded on the upper side of these samples at $2 \times 10^5$ cells (day 16) and then seeded on the lower side of the pericardium at $2 \times 10^5$ cells (day 18) in a 12-well plate. These samples were incubated in EGM-2 medium supplemented with TGF-$\beta$1 (2.5 ng/mL) and BMP-4 (2.5 ng/mL), and these pericardial samples were cultured until day 28.

### *Immunofluorescence staining of recellularized pericardium*

Native, decellularized, and decellularized porcine pericardia treated with α-galactosidase in combination with PNGase-F, which had been seeded with ADSCs and HUVECs, were fixed in 4% paraformaldehyde solution and sectioned into 5 $\mu$m on microtome. Paraffin sections were processed for H&E and immunefluorescence (IF) staining. IF staining was performed using embedded sections and deparaffinized. Tissue samples were incubated in antigen retrieval buffer (10 mM citrate buffer, pH 6.0) at 95°C for 10 min. Tissue sections were then blocked with 5% blocking serum. Tissue slides were then incubated with primary antibodies for vimentin (ab16700, Abcam, dilution 1:200), calponin (ab227661, Abcam, dilution 1:100), fibronectin (F0916, sigma, dilution 1:100), and CD31 (ab182981, Abcam, dilution 1:2000) at 4°C overnight and were washed 3 times with PBST. The tissues were then incubated with antirabbit secondary antibody conjugated with Alexa Fluor 488 (A11008, Invitrogen, 1:500) for 2 h and antimouse secondary antibody conjugated with Alexa Fluor 488 (AB150113, Invitrogen, 1:500) for 2 h, and were rinsed 3 times in PBST. Nuclei were counterstained with DAPI (Invitrogen, 1:1000) for 1 min. The sections were

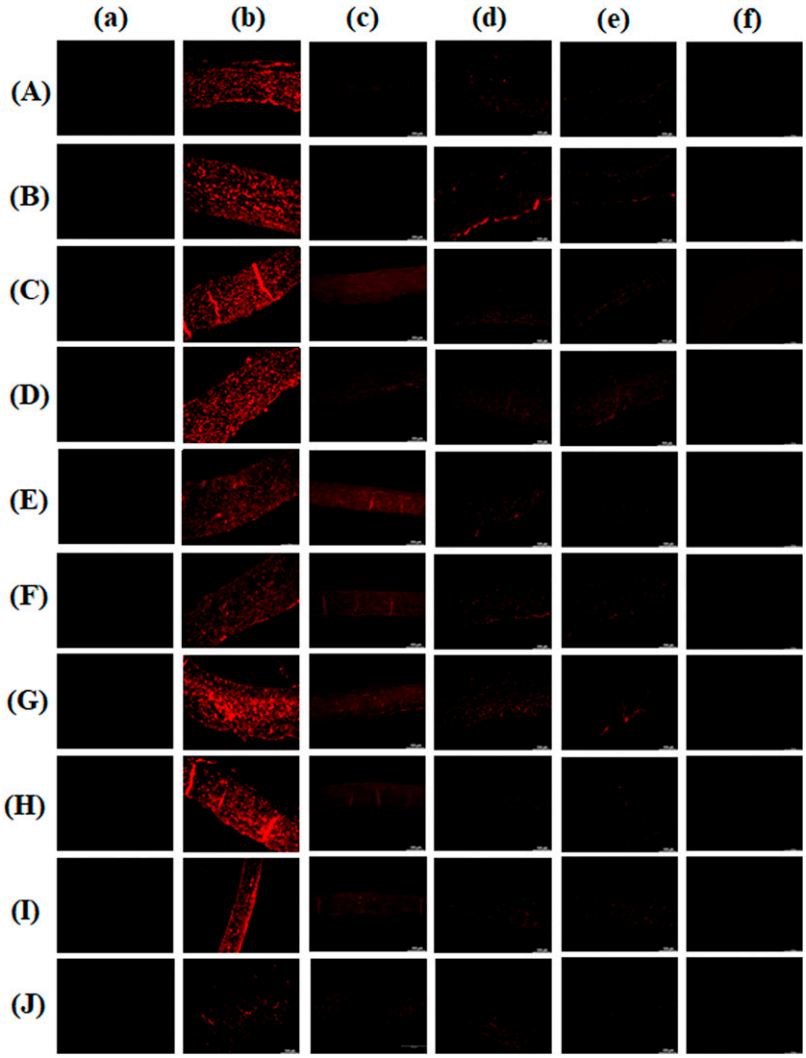


**FIG. 5.** Expression of lectins on decellularized pericardium with or without enzymatic treatment. **(a–b)** Native porcine pericardium and **(c–f)** Tx + SDS-decellularized porcine pericardium. **(a–f)** The samples were treated with or without 0–1000 unit/mL PNGase-F, respectively, in the absence and presence of α-galactosidase (0.1–0.2 unit/mL) for 24 h. Negative control **(a)**, native **(b)**, decellularized **(c)**, α-galactosidase 0.1 **(d)**, α-galactosidase 0.2 **(e)**, and α-galactosidase 0.1 + PNGase-F 2000 **(f)** porcine pericardium samples were cut longitudinally and stained with Jacalin **(A)**, MAL-I **(B)**, WGA **(C)**, RCA-I **(D)**, GSL **(E)**, ECA **(F)**, PNA **(G)**, SBA **(H)**, WFA **(I)**, and DSL **(J)**. Each sample of carbohydrate-binding lectins was stained red. The magnification used was ×200. Tx, Triton X-100; SDS, sodium dodecyl sulfate.

washed 3 times with PBST, and stained sections were imaged using an inverted fluorescence microscope (DMI4000B, Leica, Germany). Stained images were obtained using Application Suite X Image Viewer (Leica).

## Results

### *Histology and biomechanical property in decellularized porcine pericardium with enzymatic digestion*

Porcine pericardial tissues were processed according to our developed decellularization protocol using 0.25% SDS + Triton X-100 and subjected to a multistep method using hypotonic, isotonic, and hypertonic buffer solutions (Supplementary Fig. S1) (Supplementary Fig. S2). Separate samples were prepared for each enzyme treatment, which was treated with or without 0–2000 unit/mL PNGase-F, respectively, in the absence and presence of α-galactosidase (0.1–0.2 unit/mL) for 24 h. H&E staining was used to examine the fiber structure, such as the collagen fiber pattern, structural loosening, and the presence of cells, and in all cases, a normal collagen structure similar to that of fresh tissue was observed regardless of enzyme concentration (Fig. 1) (Supplementary Fig. S3).

Biomechanical properties were determined with a uniaxial tensile test and a permeability test. The tensile stress and permeability test showed no significant differences between native porcine tissue and the differently (0–1000 unit/mL) PNGase-F-treated porcine tissue and differently (0.1–0.2 unit/mL) α-galactosidase-treated porcine tissue and PNGase-F and α-galactosidase both treated porcine tissue (Fig. 2). These findings suggested that the effects of PNGase-F/α-galactosidase treatment concentration and combination were not reflected in the biomechanical properties of the porcine pericardium.

### *Lectin histochemistry and lectin binding assay in decellularized porcine pericardium with enzyme digestion*

In xenotransplantation, carbohydrate components such as lectins play a significant role, with elevated lectin levels being closely associated with immune rejection. We investigated the effects of enzymatic digestion using PNGase-F and α-galactosidase in fresh pericardium on carbohydrate removal through the expression of lectins. Native tissue, tissues treated with varying concentrations of PNGase-F and α-galactosidase, and tissues treated with both PNGase-F and α-galactosidase were stained with Jacalin, MAL-I, WGA, RCA-I, GSL, ECA, PNA, SBA, WFA, and DSL. Each enzymatic treatment showed a decrease in lectin expression as the concentration increased, indicating effective removal of carbohydrates in lectin histochemistry. In addition, when α-galactosidase and PNGase-F were treated together, a more significant reduction in lectin expression was observed, indicating that both α-Gal and non-α-Gal epitopes were more effectively removed (Fig. 3).

To quantitatively determine the expression of MAL-I, WGA, RCA-I, GSL, ECA, PNA, SBA, WFA, and DSL, a lectin binding assay for native, PNGase-F (0–1000 unit/mL), and α-galactosidase (0.1–0.2 unit/mL), α-galactosidase 0.1 + PNGase-F 1000 was performed. PNGase-F treatment significantly inhibited lectin binding levels in a concentration-dependent manner. Interestingly, when α-galactosidase was treated simultaneously with PNGase-F at the same concentration, most lectins showed reduced binding more synergistically compared to PNGase-F treatment alone (Fig. 4).

We applied an additional decellularization protocol and observed through histochemical staining that the group treated with α-galactosidase 0.1/PNGase-F 2000 showed the most effective removal of lectin binding level (Fig. 5).

### In vitro *evaluation of recellularized porcine pericardium with ADSC and HUVEC coculture*

Histological observation in both ADSC and HUVEC seeded onto modified pericardium. First, decellularized porcine pericardium was treated with or without 2000 unit/mL PNGase-F, respectively, in the absence and presence of α-galactosidase (0.1 unit/mL) for 24 h. Native, decellularized, and decellularized-α-galactosidase/PNGase-F combination pericardial samples were coated with a fibrin mesh + heparin (Fb + H) and incubated with VEGF (Fb + H + VEGF). Then, all modified pericardial samples were seeded with human ADSCs and subsequently with HUVECs. These modified pericardial samples were incubated on day 7 and on day 28, and these samples were stained with H&E. In the native, decellularized, and decellularized-α-galactosidase/PNGase-F combination pericardial samples, the tissue structure was preserved in all groups. In the group treated with and without the α-galactosidase/PNGase-F combination after decellularization, cell infiltration was observed. In the decellularized tissue, cells were observed to line the outer edges of the tissue at day 7, while cells were observed to infiltrate into the tissue by day 28. In the α-galactosidase/PNGase-F combination-treated group, cells had already infiltrated into the tissue by day 7, and by day 28, a

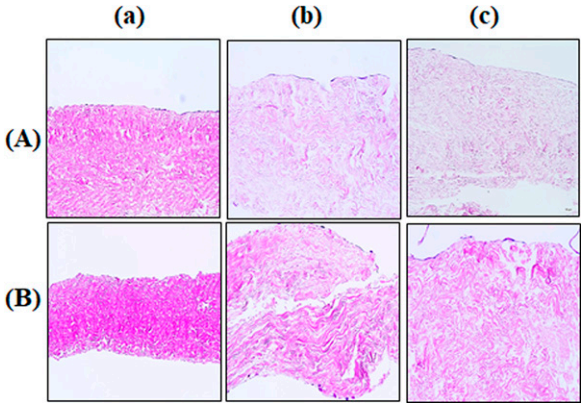


**FIG. 6.** Histological observation in both ADSC and HUVEC seeded onto modified pericardium. The decellularized porcine pericardium was treated with or without 2000 unit/mL PNGase-F, respectively, in the absence and presence of α-galactosidase (0.1 unit/mL) for 24 h. Native **(a)**, decellularized **(b)**, and decellularized-α-galactosidase/PNGase-F combination **(c)** pericardium samples coated with a fibrin mesh + heparin (Fb + H) and coated pericardium incubated with VEGF (vascular endothelial growth factor, Fb + H + VEGF). Then, all modified pericardium samples were seeded with human ADSCs and subsequently with human umbilical endothelial cells (HUVECs), and these modified pericardium samples were incubated on day 7 **(A)** and on day 28 **(B)**, and these samples were stained with H&E. H&E stains were imaged using a microscope. The magnification used was ×200. Fb: fibrin-coated pericardium; Fb + H + VEGF: pericardium coated with fibrin, heparin, and VEGF.

significant number of cells were found to infiltrate into the tissue (Fig. 6).

Immunofluorescence staining in both ADSCs and HUVECs seeded onto modified pericardium. Native, decellularized, and decellularized-α-galactosidase/PNGase-F combination samples were incubated for 7 days and 28 days, and these samples were stained with vimentin, which is a marker of mesenchymal cells. Vimentin-positive cells were present on the surface of the pericardium on day 7. On day 28, a significant number of cells were observed to line the surface and penetrate deeper into the tissue. In particular, the decellularized-α-galactosidase/PNGase-F combination sample showed faster mesenchymal cell infiltration into the tissue, leading to accelerated recellularization (Fig. 7).

Calponin is an intermediate marker indicating cell differentiation into vascular smooth muscle cells. On day 7 of culture, minimal stainings were observed. On day 28, calponin-positive cells began to appear on the surface of the pericardium. In the decellularized-α-galactosidase/PNGase-F combination sample, calponin-positive signals were observed inside the tissue, suggesting that the infiltrating cells are differentiated into smooth muscle cells (Fig. 8).

Fibronectin staining serves as a key component of the ECM, promoting cell attachment and regeneration. Intense fibronectin staining was observed, and stronger signals in tissue were detected in the decellularized group cultured for 28 days compared to 7 days, as well as in the decellularized group treated with both α-galactosidase and PNGase-F simultaneously (Fig. 9).

CD31 positivity indicates the expression of CD31 (platelet endothelial cell adhesion molecule-1, PECAM-1) protein in cells or tissues. CD31 is primarily expressed in endothelial cells and some immune cells, playing a critical role in angiogenesis, cell-cell adhesion, and inflammatory responses. Similar to the staining of other markers, a strong signal was observed within the tissue on day 28 in the decellularized-α-galactosidase/PNGase-F combination group, suggesting that new blood vessels are forming in the recellularized graft (Fig. 10), (Supplementary Fig. S4).

## Discussion

Significant research has been conducted to develop an ideal tissue-engineered heart valve by selecting suitable tissues to serve as scaffolds for optimal valve structures. In the case of xenogeneic tissues, efforts have focused on appropriately removing cells that may trigger immune responses while minimizing damage to the ECM.[9,10] Decellularization protocols have been developed to process the ECM into an immunologically tolerable state while preserving its functionality. Generally, decellularization is achieved using chemical methods (alkaline/acid, detergents, alcohols), physical methods (electroporation, pressurization, and freeze/thaw), and biological methods (enzymes, etc.).[1,11] The removal of nucleic acid residues is crucial in all decellularization processes because these

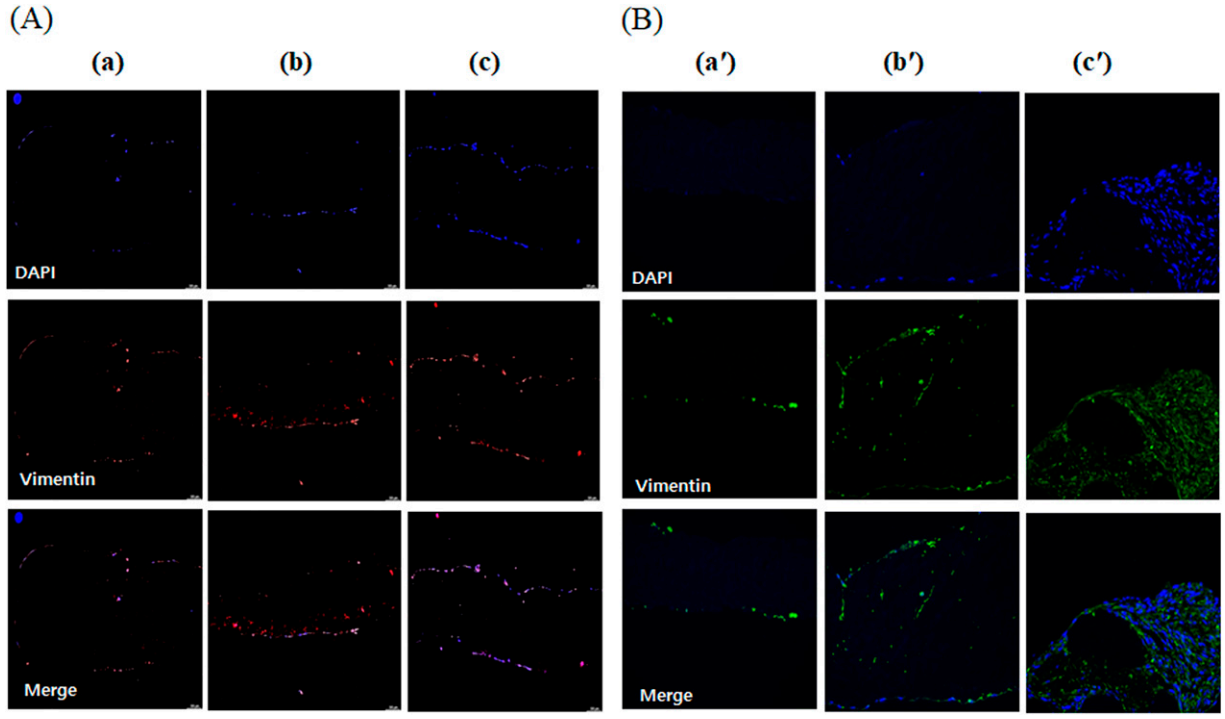


**FIG. 7.** Immunofluorescence staining of vimentin in ADSC and HUVEC coculture on to modified pericardium. The decellularized porcine pericardium was treated with or without 2000 unit/mL PNGase-F, respectively, in the absence and presence of α-galactosidase (0.1 unit/mL) for 24 h. All porcine pericardium samples modified with fibrin, heparin, and VEGF (Fb + H + VEGF). Then, all modified pericardium samples were seeded with ADSCs and HUVEC. Native **(a, a′)**, decellularized **(b, b′)**, and decellularized-α-galactosidase/PNGase-F combination **(c, c′)** samples were incubated on day 7 **(A)** and on day 28 **(B)**, and these samples were stained with vimentin. Fluorescence signals of vimentin were determined using a fluorescence microscope. Cell nuclei were stained with 4′,6-diamidino-2-phenylindole (DAPI). The magnification used was ×200.

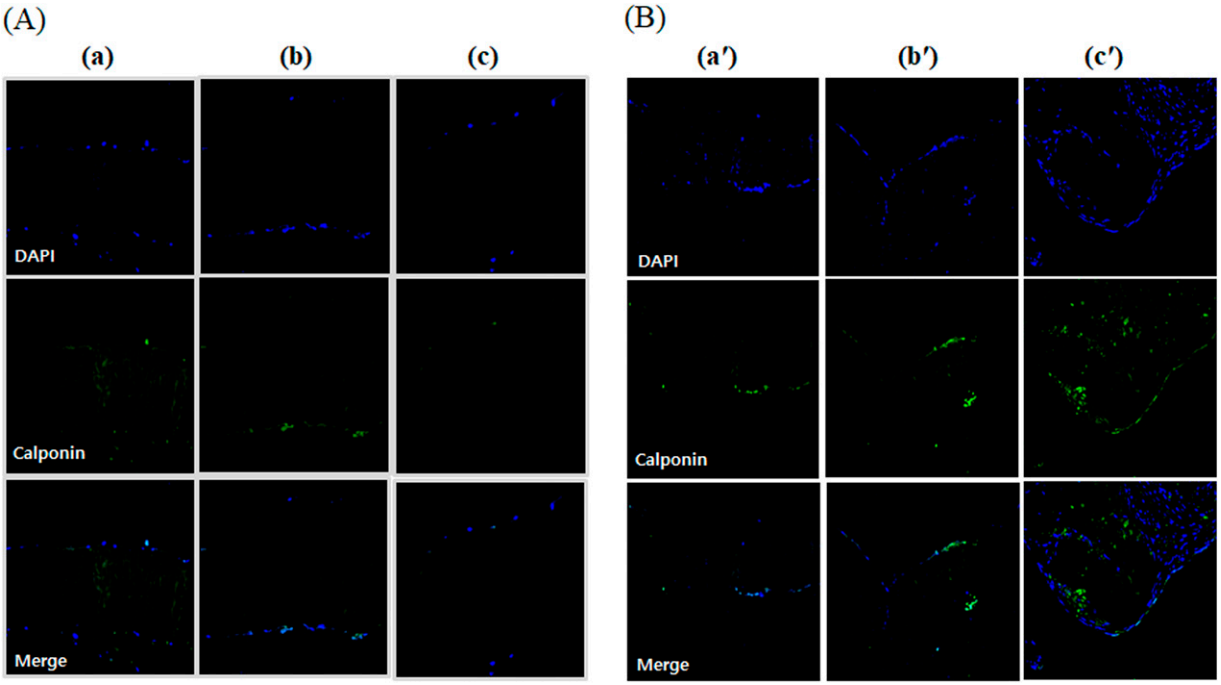


**FIG. 8.** Immunocytochemical staining of calponin in ADSC and HUVEC coculture onto modified pericardium. The decellularized porcine pericardium was treated with or without 2000 unit/mL PNGase-F, respectively, in the absence and presence of α-galactosidase (0.1 unit/mL) for 24 h. All porcine pericardium samples were modified with fibrin, heparin, and VEGF (Fb + H + VEGF). Then, all modified pericardium samples were seeded with ADSCs and HUVEC. Native **(a, a′)**, decellularized **(b, b′)**, and decellularized-α-galactosidase/PNGase-F combination **(c, c′)** samples were incubated on day 7 **(A)** and on day 28 **(B)**, and these samples were stained with calponin. Fluorescence signals of calponin were determined using a fluorescence microscope. Cell nuclei were stained with 4′,6-diamidino-2-phenylindole (DAPI). The magnification used was ×200.

residues tend to adhere to ECM and attract circulating calcium salts, leading to calcification and subsequent tissue degeneration. Therefore, during tissue decellularization, proteolytic enzymes are used to break down proteins and effectively separate cellular components from the connective tissue.

In particular, when using pig or bovine pericardial tissues, it is necessary to effectively remove α-Gal (xenoepitope), which induces xenogeneic immune rejection in humans.[5] We have previously developed a decellularization protocol incorporating an α-galactosidase, which has been utilized to create artificial pericardial pulmonary valves. These valves have been successfully applied in clinical practice, and the outcomes to date have been satisfactory.[6,12] However, it has been found that the presence of non-Gal antigens (Neu5Gc) in the GalT-KO area does not trigger hyperacute xenorejection but can mediate acute graft damage to both vascularized organs and cellular grafts in xenotransplantation.[13] Furthermore, anti-non-Gal antibodies will be induced upon xenograft or tissue, and it can be anticipated, analogously to the human allo-situation, that these will have an impact on xenograft or tissue survival and durability. In xenotransplantation, lectins are carbohydrate-binding protein components that are deeply involved in immune rejection, and increased lectin levels are closely associated with immune rejection. The effect of enzymatic treatment using PNGase-F on carbohydrate removal was investigated by analyzing lectin expression. In our previous studies, we demonstrated that combining decellularization with PNGase-F treatment effectively removes non-Gal antigens without affecting the mechanical stability of the tissue.[14] The removal of non-Gal antigens, such as Neu5Gc, primarily requires deglycosylation treatment, which effectively eliminates carbohydrates from *N*- and *O*-glycans. In this study, as the concentration of PNGase-F increased, the binding signals for all lectins decreased, and when combined with a low concentration of α-galactosidase, a synergistic reduction in lectin binding was observed without altering the mechanical properties. The combination of PNGase-F and α-galactosidase effectively removes xenoantigenic carbohydrates from porcine pericardium, demonstrating the potential to reduce immunogenicity. Lectin binding xenoantigenic carbohydrates removal was more effective when decellularization was performed. The absence of cells in the decellularized xenograft tissue was confirmed using H&E staining and DAPI staining. Since it is essential to completely remove antigens that can trigger graft-versus-host reactions, we propose a novel chemical-based decellularization method that effectively eliminates residual cells while preserving the structural integrity of the tissue.

The decellularized xenograft scaffold is recellularized with host cells in an *in vivo* environment while withstanding hemodynamic stresses. Tissue analysis of the xenografted valve revealed the infiltration of valvular interstitial cells (VICs) and valvular endothelial cells (VECs) in the valve cusps. VECs form a nonthrombotic monolayer on the valve surface, playing a critical role in the hemodynamic properties of the valve.[15] VICs are involved in the remodeling of the ECM of the valve, ensuring tissue durability and growth characteristics.[16] A significant presence of myofibroblast-

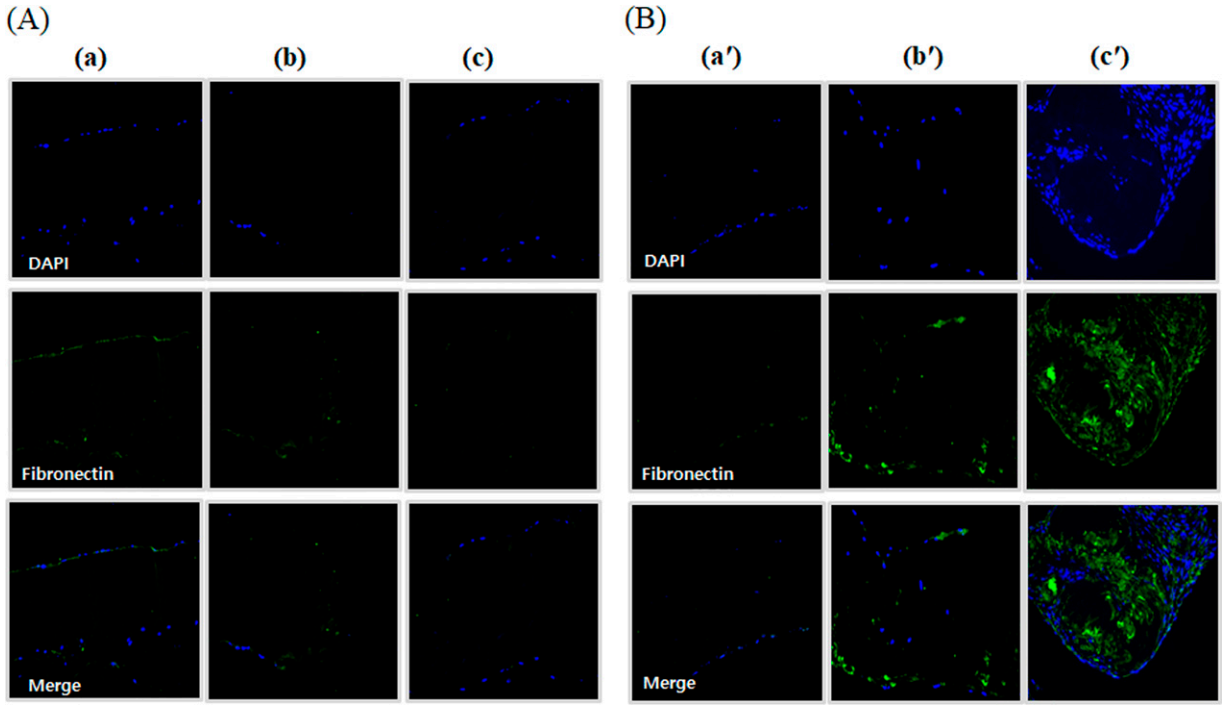


**FIG. 9.** Immunocytochemical staining of fibronectin in ADSC and HUVEC coculture onto modified pericardium. The decellularized porcine pericardium was treated with or without 2000 unit/mL PNGase-F, respectively, in the absence and presence of α-galactosidase (0.1 unit/mL) for 24 h. All porcine pericardium samples were modified with fibrin, heparin, and VEGF (Fb + H + VEGF). Then, all modified pericardium samples were seeded with ADSCs and HUVEC. Native **(a, a′)**, decellularized **(b, b′)**, and decellularized-α-galactosidase/PNGase-F combination **(c, c′)** samples were incubated on day 7 **(A)** and on day 28 **(B)**, and these samples were stained with fibronectin. Fluorescence signals of fibronectin were determined using a fluorescence microscope. Cell nuclei were stained with 4′,6-diamidino-2-phenylindole (DAPI). The magnification used was ×200.

like VICs, which were positive for α-smooth muscle actin (α-SMA) and vimentin, was also observed.[17] This demonstrates the potential of decellularized xenograft valves to undergo recellularization and differentiation in an *in vivo* environment through blood flow.

However, when a decellularized xenograft valve tissue is implanted to enable host cell recellularization, the absence or delayed recruitment of cells capable of repairing and remodeling the ECM during the valvular cycle may lead to tissue failure or degradation due to valve tissue damage. *In situ* recellularization has been less successful in clinical settings compared to preclinical studies.[18,19] While recellularization of decellularized grafts has been observed, it was often partial, and in some cases, the repopulated cells appeared to be inflammatory rather than phenotypically appropriate valve cells. Thus, another potential approach could involve seeding MSCs on the surface of decellularized engineered valve tissue *in vitro* to induce recellularization.[20] If the speed of recellularization could be further enhanced *in vivo*, or if a xenogeneic tissue valve prerecellularized *in vitro* could be implanted to accelerate the recellularization process, it would be possible to create a more biocompatible and regenerative valve tissue within the human body.[17,20]

For *in vitro* recellularization, it is essential to use an appropriate cell source and provide conditioning signals in a bioreactor to induce cell proliferation and differentiation. Various cell sources have been studied for heart valve tissue engineering, and among them, we utilized MSCs. MSCs possess self-renewal and differentiation capabilities and can be easily obtained from various tissues such as bone marrow, adipose tissue, placenta, and umbilical cord. MSCs interact with surrounding tissues, differentiate into tissue-specific cells, reduce inflammatory cytokines, and promote new blood vessel formation, making them a promising cell type for repopulating decellularized scaffolds.[21] In this study, human adipose tissue-derived MSCs were utilized as a cell source to induce recellularization. The process of attaching MSCs to scaffolds is facilitated through interactions between specific cellular integrins and various ECM proteins. We coated decellularized pericardium with fibrin to enhance cell adhesion, proliferation, and differentiation. In addition, we incorporated heparin and VEGF to further promote recellularization.[8]

Fibronectin mediates various cell interactions with the ECM, playing a crucial role in cell adhesion, migration, growth, and differentiation.[22] When decellularized tissue treated with a combination of α-galactosidase and PNGase-F was cocultured with MSCs and HUVECs, the expression of fibronectin was elevated, suggesting that MSCs infiltrated the tissue more rapidly and abundantly.[23] Fibronectin may have originated from the serum contained in the culture medium or from the MSCs. Some studies have suggested that preimplant conditioning with fibronectin alone or in combination with other growth factors can enhance *in situ* recellularization. In this study, we confirmed that using fibrin and heparin-VEGF in a coculture of HUVECs and MSCs

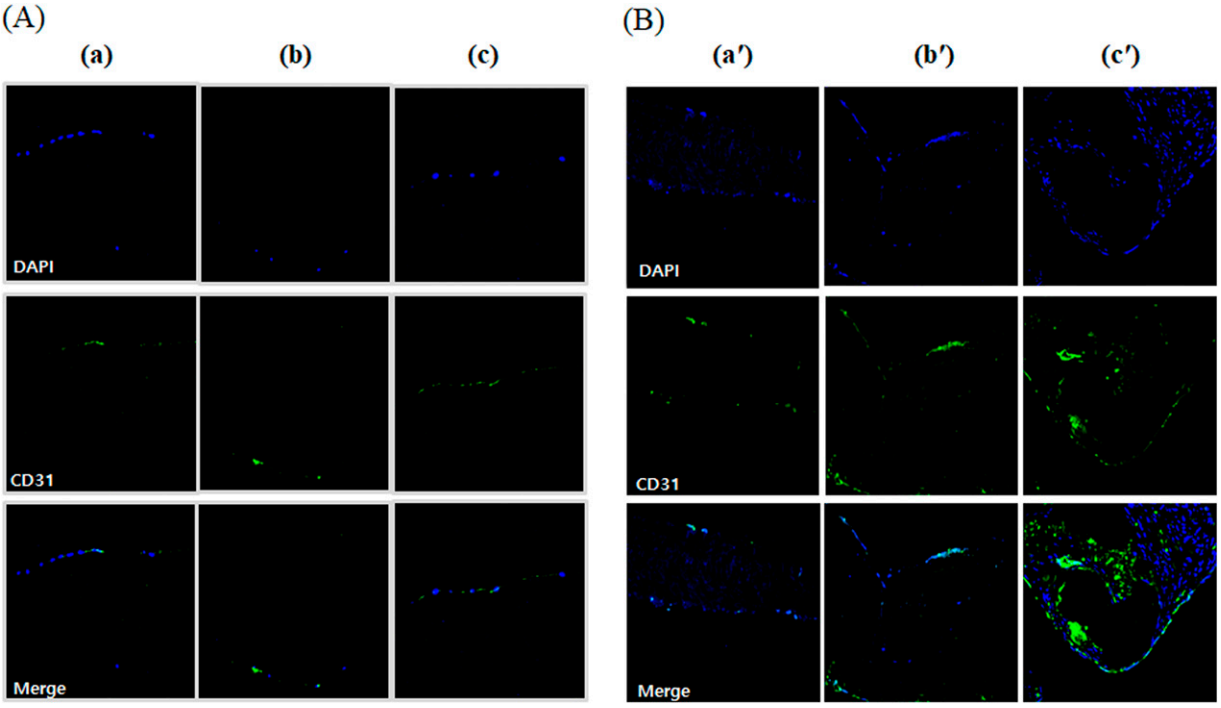


**FIG. 10.** Immunocytochemical staining of CD31 in ADSC and HUVEC coculture onto modified pericardium. The decellularized porcine pericardium was treated with or without 2000 unit/mL PNGase-F, respectively, in the absence and presence of α-galactosidase (0.1 unit/mL) for 24 h. All porcine pericardium samples were modified with fibrin, heparin, and VEGF (Fb + H + VEGF). Then, all modified pericardium samples were seeded with ADSCs and HUVEC. Native **(a, a′)**, decellularized **(b, b′)**, and decellularized-α-galactosidase/PNGase-F combination **(c, c′)** samples were incubated on day 7 **(A)** and on day 28 **(B)**, and these samples were stained with CD31. Fluorescence signals of CD31 were determined using a fluorescence microscope. Cell nuclei were stained with 4′,6-diamidino-2-phenylindole (DAPI). The magnification used was ×200.

can promote increased cell attachment for the recellularization of decellularized scaffolds.[24]

Through vimentin staining, we confirmed that MSCs migrated into the tissue, and the activation of interstitial cells was initiated, indicating the beginning of tissue remodeling. Particularly, as myofibroblasts can also exhibit vimentin positivity, this suggests that it represents an early stage of ECM remodeling and tissue repair. However, to confirm whether these cells are in the early stages of myofibroblasts, it is necessary to check for coexpression of α-SMA positivity.

Calponin staining suggested that MSCs interacted with the surrounding ECM and transitioned into myofibroblasts, exhibiting a mature smooth muscle cell phenotype. This was particularly evident after 4 weeks of coculturing MSCs and HUVECs on tissue treated with α-galactosidase and PNGase-F, where calponin expression was significantly increased. These findings indicate that multipotential stem cells undergo recellularization at the valve site and differentiate into mature cell phenotypes.

However, excessive activation of myofibroblasts can lead to tissue fibrosis and valve stiffening, which may result in functional impairment over the long term.

When the graft achieves sufficient endothelialization in the human body and therapeutic angiogenesis occurs, the incidence of thrombosis is reduced. In addition, paracrine signaling promotes recellularization, enabling differentiation into improved tissue structures. Previous studies have observed an increase in markers expressed in vascular endothelium, CD31, through the coculture of HUVECs and MSCs, demonstrating that coculture is effective for the rapid endothelialization of vascular substrates.[25,26] This finding was also replicated in our study. Thus, xenografts recellularized with MSCs can regulate the host immune response, enabling effective tissue remodeling, delaying the biodegradation process, and extending the survival of the tissue until successful ECM replacement is achieved in the recipient.

Compared with recent TRICOL decellularization based on osmotic shock, detergents, and nuclease treatment,[27] our decellularization protocol using SDS and Triton X-100 through a multistep method with hypotonic, isotonic, and hypertonic buffer solutions was developed without nuclease and successfully commercialized due to its economic feasibility and mass productivity. Lately, decellularization and subsequent recellularization particularly focus on the obstacles and unresolved issues that must be overcome toward optimal tissue engineering.[28] The glycans with terminal α-Gal and Neu5Gc are known to play a major role in xenoimmunogenicity, ultimately leading to graft rejection.[29] Similar to our results, the decellularization protocols were revised in combination with enzymatic deglycosylation to reduce xenoimmunogenicity, by means of cells, carbohydrates, and primarily α-Gal epitope removal, and decellularized xenografts treated with PNGase-F resulted in potentially reduced immunogenicity with mechanical stability.[30]

In the development of tissue-engineered heart valves, strategies to recellularize the entire valve, including decellularized

xenoantigen-free scaffolds, with an appropriate cell population face numerous challenges. This experiment suggests the potential for promoting recellularization of xenogeneic valvular tissue *in vitro* prior to transplantation. In this study, we confirmed the extent of recellularization through immunohistochemical staining; however, it is necessary to further quantify this process and evaluate the degree of differentiation and reconstruction using various additional markers. Furthermore, measuring ECM proteins involved in tissue reconstruction is crucial to elucidating the processes underlying tissue changes. Further studies are needed to evaluate the immune response of such recellularized tissues *in vivo*, as well as to investigate how well the recellularized cells can sustain growth and differentiation under stress conditions.

In conclusion, we have successfully produced xenoantigen-free scaffolds by demonstrating the safety and the synergistic effect of α-galactosidase and PNGase-F treatments and proved effective recellularization for the xenoantigen-free scaffolds not previously reported in the literature.

### Authors' Contributions

J.K.Y.: Contributed to the conceptualization, generating figures of the article, writing of the article. S.Y.K.: Contributed to the conceptualization, generating figures of the article, and writing of the article. S.Kim.: Contributed to the generating figures of the article. K.M.L.: Contributed to the generating figures of the article. S.Ko.: Contributed to the generating figures of the article. G.B.K.: Contributed to the conceptualization, and writing of the article. H.G.L.: Contributed to the conceptualization, generating figures of the article, and writing of the article. Y.J.K.: Contributed to the conceptualization, and writing of the article.

### Disclosure Statement

No competing financial interests exist.

### Funding Information

This research was supported and funded by SNUH Lee Kun-hee Child Cancer & Rare Disease Project, Republic of Korea (grant number: 25C-022-0100).

### Supplementary Material

Supplementary Figures

### Reference

1. Neishabouri A, Khaboushan AS, Daghigh F, et al. Decellularization in tissue engineering and regenerative medicine: Evaluation, modification, and application methods. Front Bioeng Biotechnol 2022;10:805299.
2. Lim HG, Kim SH, Choi SY, et al. Anticalcification effects of decellularization, solvent, and detoxification treatment for genipin and glutaraldehyde fixation of bovine pericardium. Eur J Cardiothorac Surg 2012;41(2):383–390.
3. Nam J, Choi SY, Sung SC, et al. Changes of the structural and biomechanical properties of the bovine pericardium after the removal of α-Gal epitopes by decellularization and α-Galactosidase treatment. Korean J Thorac Cardiovasc Surg 2012;45(6):380–389.
4. Lim HG, Kim GB, Jeong S, et al. Development of a next-generation tissue valve using a glutaraldehyde-fixed porcine aortic valve treated with decellularization, α-galactosidase, space filler, organic solvent and detoxification. Eur J Cardiothorac Surg 2015;48(1):104–113.
5. Choi SY, Jeong HJ, Lim HG, et al. Elimination of alpha-gal xenoreactive epitope: Alpha-galactosidase treatment of porcine heart valves. J Hear Valve Dis 2012;21(3):387–397.
6. Kim GB, Kwon BS, Lim HG. First in human experience of a new self-expandable percutaneous pulmonary valve implantation using knitted nitinol-wire and tri-leaflet porcine pericardial valve in the native right ventricular outflow tract. Catheter Cardiovasc Interv 2017;89(5):906–909.
7. Lim HG, Choi SY, Yoon EJ, et al. In vivo efficacy of Alpha-Galactosidase as possible promise for prolonged durability of bioprosthetic heart valve using Alpha1,3-Galactosyltransferase knockout mouse. Tissue Eng Part A 2013;19(21–22):2339–2348.
8. Filova E, Steinerova M, Travnickova M, et al. Accelerated *in vitro* recellularization of decellularized porcine pericardium for cardiovascular grafts. Biomed Mater 2021;16(2):025024.
9. Nelson CM, Bissell MJ. Of extracellular matrix, scaffolds, and signaling: Tissue architecture regulates development, homeostasis, and cancer. Annu Rev Cell Dev Biol 2006; 22(1):287–309.
10. Badylak SF. The extracellular matrix as a biologic scaffold material. Biomaterials 2007;28(25):3587–3593.
11. Badylak SF, Taylor D, Uygun K. Whole-organ tissue engineering: Decellularization and recellularization of three-dimensional matrix scaffolds. Annu Rev Biomed Eng 2011; 13(1):27–53.
12. Kim GB, Song MK, Bae EJ, et al. Successful feasibility human trial of a new self-expandable percutaneous pulmonary valve (Pulsta Valve) Implantation using knitted nitinol wire backbone and trileaflet α-gal–free porcine pericardial valve in the native right ventricular outflow tract. Circ: Cardiovasc Interv 2018;11(6):e006494.
13. Breimer ME. Gal/non-Gal antigens in pig tissues and human non-Gal antibodies in the GalT-KO era1. Xenotransplantation 2011;18(4):215–228.
14. Kim SY, Kim GB, Lim HG, et al. Strategies beyond decellularization for optimal tissue engineering of cardiac xenografts. J Biomed Res Environ Sci 2024;5(9):1253–1265.
15. Butcher JT, Nerem RM. Valvular endothelial cells regulate the phenotype of interstitial cells in co-culture: Effects of steady shear stress. Tissue Eng 2006;12(4):905–915.
16. Liu AC, Joag VR, Gotlieb AI. The emerging role of valve interstitial cell phenotypes in regulating heart valve pathobiology. Am J Pathol 2007;171(5):1407–1418.
17. Hennessy RS, Go JL, Hennessy RR, et al. Recellularization of a novel off-the-shelf valve following xenogenic implantation into the right ventricular outflow tract. PLoS One 2017;12(8):e0181614.
18. James IA, Yi T, Tara S, et al. Hemodynamic characterization of a mouse model for investigating the cellular and molecular mechanisms of neotissue formation in tissue-engineered heart valves. Tissue Eng Part C Methods 2015;21(9):987–994.
19. Perri G, Polito A, Esposito C, et al. Early and late failure of tissue-engineered pulmonary valve conduits used for right ventricular outflow tract reconstruction in patients with congenital heart disease. Eur J Cardiothorac Surg 2012;41(6): 1320–1325.

20. Syedain ZH, Bradee AR, Kren S, et al. Decellularized tissue-engineered heart valve leaflets with recellularization potential. Tissue Eng Part A 2013;19(5–6):759–769.
21. Duan B, Hockaday LA, Das S, et al. Comparison of mesenchymal stem cell source differentiation toward human pediatric aortic valve interstitial cells within 3d engineered matrices. Tissue Eng Part C Methods 2015;21(8):795–807.
22. Pankov R, Yamada KM. Fibronectin at a glance. J Cell Sci 2002;115(Pt 20):3861–3863.
23. Dinesh NEH, Campeau PM, Reinhardt DP. The integral role of fibronectin in skeletal morphogenesis and pathogenesis. Matrix Biol 2024;134:23–29.
24. Assmann A, Delfs C, Munakata H, et al. Acceleration of autologous *in vivo* recellularization of decellularized aortic conduits by fibronectin surface coating. Biomaterials 2013; 34(25):6015–6026.
25. Verseijden F, Sluijs S V, Pavljasevic P, et al. Adult human bone marrow– and adipose tissue–derived stromal cells support the formation of prevascular-like structures from endothelial cells *in vitro*. Tissue Eng Part A 2010;16(1):101–114.
26. Joshi A, Xu Z, Ikegami Y, et al. Co-culture of mesenchymal stem cells and human umbilical vein endothelial cells on heparinized polycaprolactone/gelatin co-spun nanofibers for improved endothelium remodeling. Int J Biol Macromol 2020;151:186–192.
27. Zouhair S, Sasso ED, Tuladhar SR, et al. A comprehensive comparison of bovine and porcine decellularized pericardia: New insights for surgical applications. Biomolecules 2020; 10(3):371.
28. Hussein K, Korossis S, Iop L. Editorial: Tissue and organ decellularization strategies in regenerative medicine; recent advances, current translational challenges, and future directions. Front Bioeng Biotechnol 2023;11:1201041.
29. Morticelli L, Rossdam C, Cajic S, et al. Genetic knockout of porcine GGTA1 or CMAH/GGTA1 is associated with the emergence of neo-glycans. Xenotransplantation 2023; 30(4):e12804.
30. Findeisen K, Morticelli L, Goecke T, et al. Toward acellular xenogeneic heart valve prostheses: Histological and biomechanical characterization of decellularized and enzymatically deglycosylated porcine pulmonary heart valve matrices. Xenotransplantation 2020;27(5):e12617.

Address correspondence to:
*Hong-Gook Lim, MD, PhD*
*Department of Thoracic and Cardiovascular Surgery*
*Seoul National University Hospital*
*Seoul National University College of Medicine*
*101 Daehak-ro*
*Jongno-gu*
*Seoul 03080*
*South Korea*

*E-mail:* hongklim@hanmail.net

*Received: January 16, 2025*
*Accepted: May 14, 2025*
*Online Publication Date: August 20, 2025*